Engineering Chemistry
ISSN: 2813-6535, Vol. 4, pp 17-31
doi:10.4028/p-XakNe1

Submitted: 2022-11-11
Revised: 2023-04-03
Accepted: 2023-04-03
Online: 2023-08-11

A Review: Membrane Reactor for Hydrogen Production: Modeling and Simulation

Alaa Hasan Kassi[1,a*], Tahseen A. Al-Hattab[2,b*]

[1,2]Chemical Engineering Department, Babylon University, Babylon, Iraq.

[a]alaa90eng@gmail.com, [b]alhattab.t@gmail.com

Keywords: H_2 Production, Modeling & Simulation, Membrane Reactor (MR).

Abstract. A membrane reactor is a multifactional vessel used for H_2 production. Hydrogen's three spectrum colors are dependent on carbon present. Two types of membrane with high permeability to hydrogen (polymeric and metallic). Hydrogen is produced in two systems: conventional reactors and membrane reactors (which separate and purify hydrogen in a single vessel). There are many types of membrane reactors according to design (catalytic membrane reactor (CMR), fixed bed reactor (FBMR), fluidized bed reactor (FBMR), etc. The transport mechanism of H_2 through the membrane by a "sorption-diffusion mechanism" and the government equations that are used for membrane reactor modeling and simulation, such as continuity, momentum, mass, and heat transfer equations of the CMR, and the thickness of the membrane. These equations are solved by MATLAB, COMSOL, and the Finite Element Method to simulate the MR at different parameters: rate of conversion, rate of sweep gas, temperature, pressure, rate of H_2 permeation through a membrane, and activity of the catalyst. We summarized theoretical studies for membrane reactors, including the operation conditions, type of hydrocarbon feed, type of production method, kind of catalyst, and heat effect.

Introduction

Growing interest in using hydrogen as an energy source is a result of the likelihood of climate change brought on by global warming. The majority of the world's energy demands are currently met by fossil fuels, but they regretfully emit a lot of greenhouse gases, particularly carbon dioxide. As a clean fuel that produces no CO_2 or other pollutants, hydrogen is viewed as a potential future energy source. All that is left when it burns away is water. Fuel cell technology is designed to use hydrogen to convert chemical energy directly into electrical energy [1].

Hydrogen, the most common element in the world, has only recently (within the last 300 years) been recognized as a pure, non-toxic material. Despite being an energy vector rather than a major energy source, hydrogen has some qualities that make it a good candidate for the transition to renewable energy [2].

The three hydrogen isotopes protium, deuterium, and tritium are distinct from one another. One proton and one electron make up protium, the main component of hydrogen, the simplest element. Despite being the lightest element, hydrogen has the highest energy content per unit mass among all fuels [3].

Hydrogen Method Production

Since H_2 gas cannot be found in nature as readily available molecules, it must be created from substances that already contain it. In particular, hydrocarbons and fossil fuels, or even renewable sources, can be used to make hydrogen [4]. Table 1 shows each method's benefits, drawbacks, efficiency, and cost [5].

Table 1 H_2 gas production methods from petrolume fuels with their benefits, drawbacks, performance and cost [5].

H_2 Gas Production Method	Benefits	Drawbacks	Performance [%]	Cost [$/kg]
"Steam Reforming (SR)"	"Technical advancements and current infrastructure"	"Supply of produced CO and CO_2 is unstable"	"74–85"	"2.27"
"Partial Oxidation (PO)"	"Established technology"	"Along with H_2 Production, produced heavy oils and petroleum coke"	"60–75"	"1.48"
"Autothermal Reforming" (AT)	"Well established technology & Existing infrastructure"	"Produced CO_2 as a byproduct, use of fossil fuels".	"60–75"	"1.48"

Green hydrogen is the only hydrogen fuel that is carbon-neutral because it doesn't produce any carbon during manufacturing or consumption. Grey hydrogen produces carbon during the extraction and production processes. Grey hydrogen has been developed to blue hydrogen, which seizes and stores the carbon produced during synthesis. Renewable energy sources are used to produce green hydrogen. Table 2 shows the three hues of the hydrogen spectrum, grey, blue, and green, according to their carbon output [6].

Table 2 The colour of H_2 [6].

	Grey	Blue	Green
Process	"Steam methane reforming (SMR)" "Auto-thermal reforming (ATR)"	"Carbon Capture and Storage (CCS)"	"Electrolysis"
"Source"	CH_4, gasifier coal, heavy oil	CO_2-rich stream	H_2O
Carbon leave	8.5–10 kg	0.8–4.4 kg	No emissions carbon

The hydro-treating methods used in refineries to turn raw materials into higher-value compounds (like ammonia and methanol) or feedstock for hydrogen [7]. To meet commercial demands, hydrogen separation and purification are now necessary. Membrane separation, cryogenic distillation, pressure swing adsorption, and wet and dry scrubbing are a few of the procedures used to separate hydrogen from other gases and purify it [8].

Phase change, sorbents, and their regeneration are frequently not used in membrane-based separation technologies for mixtures of gas and vapor. As a result, membrane technologies are appealing due to their advantages such as energy efficiency, operational continuity and simplicity, small footprint, simplicity in scaling up, module compactness and modularity, and environmental cost and friendliness. The energy required by membrane-based distillation procedures could be 90% lower than that of conventional techniques [9].

Types of Membrane

According to the substance used to make the membrane, which has a high permeability to hydrogen, there are two different varieties, and they are divided into two categories.

a. Polymeric Membrane

The use of polymeric membranes in commercial gas separation processes is common[10]. Polymeric glass and rubber membranes are two different types of polymer membranes. Because of their better mechanical properties and high gas selectivity, glassy polymer membranes were more practical for commercial applications than rubber polymeric membranes.

b. Metallic Membrane

Dense membranes made of palladium, platinum, nickel, and the metallic elements in bands III–V of the chemical elements have theoretically unlimited selectivity since they can transport hydrogen in a dissociated form [11].

b.1 Non-Palladium Membranes

Palladium is a particularly desirable material for metal-based membranes because it is highly selective towards hydrogen and allows for the synthesis of pure H_2. Nevertheless, palladium is expensive, and its price is erratic [12]. Thus, it was necessary to create membranes using less expensive metals. Due to their lower cost and strong hydrogen permeability, Group 5 metals with a body-centric cubic structure like tantalum, vanadium (V) and niobium (Nb) present a viable alternative to platinum. The palladium layer still required hydrogen penetration, though. When exposed to an interdiffusion between Pd and V at temperatures above 400ºC, the membranes begin to deteriorate .

b.2 Palladium (Pd) Membranes

Palladium (Pd)-based membranes for the purification of hydrogen provide the greatest selectivity and penetration due to their special permeation mechanism [13]. A dense palladium-based membrane (2–50μm) can be employed to separate pure hydrogen [14]. Palladium membranes can function at temperatures that are substantially higher than those of polymer membranes, which makes them perfect for use in membrane reactors or for removing hydrogen from gas streams at high temperatures [15].

Combining a Catalytic Reaction with the Membrane Separation Process

The membrane reactor and traditional methods for creating hydrogen are contrasted in Figure 1. Because of the separation and reaction, this is referred to as a "membrane reactor."

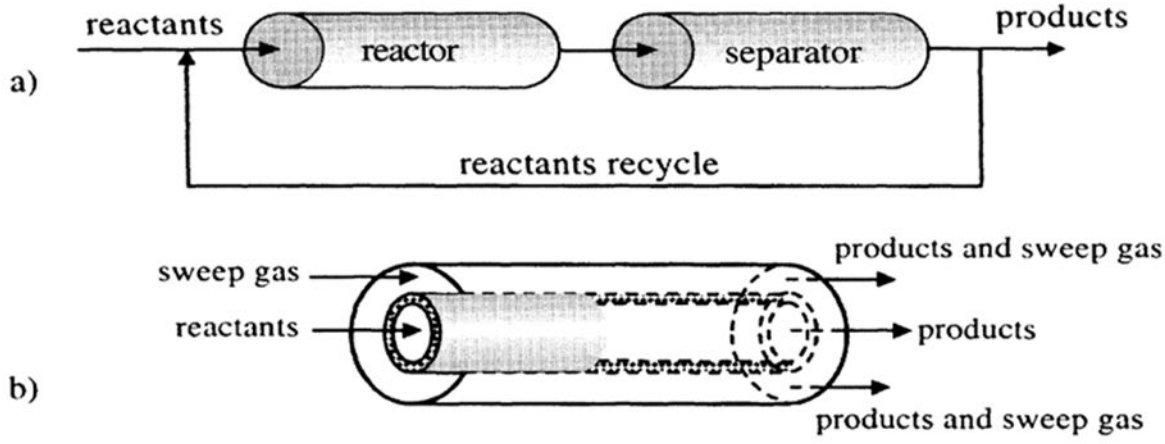

Fig. 1 (a) "A conventional reactor system" (b) "Catalytic membrane reactor system"

In Table 3. "the most common membrane reactor configurations" that have been reviewed in this[16]

Table 3 "Classification of Membrane Reactors"[16].

Acronym	Definition
"CMR	Catalytic membrane reactor"
"CNMR	Catalytic non-permselective membrane reactor"
"PBMR	Packed-bed membrane reactor"
"PBCMR	Packed-bed catalytic membrane reactor"
"FBMR	Fluidized-bed membrane reactor"
"FBCMR	Fluidized-bed catalytic membrane reactor"

Mechanisum of H_2 Transport Through the Membrane

The sorption-diffusion mechanism allows H_2 to diffuse through substantial metal obstacles. Permeation of a high partial pressure gas zone into a low partial pressure gas region happens in stages: (1) Atomic hydrogen sorption into the bulk metal (2) dissociative adsorption of H_2 at the gas-metal interface atomic hydrogen recombination to create hydrogen molecules at the metal/gas permeate interface is followed by (3) atomic hydrogen diffusion through the bulk metal membrane and (4) molecular hydrogen desorption.

The efficiency of any reactor is assessed using a variety of operational factors and design considerations, such as the ratio of reactant in the feed, temperature, pressure, membrane properties, the kind of catalyst, the rate of sweep gas, etc. Under these conditions, it seems that mathematical models are an effective tool for all kinds of reactor research and simulation [17].

Governing Equations for Membrane Reactor

The government equations that are used for membrane reactor modeling and simulation can be shown below and are used via many articles.

When developing the CFD model, consideration was given to the continuity equation (Eq.1), momentum equation (Eq.2), and mass transfer equation (Eq.3) [18].

$$\nabla(\rho f.\,\varepsilon.\,u) = Si \tag{1}$$

$$\nabla(\rho f.\,u) = -\nabla P - \beta u + \nabla\tau + \rho f g \tag{2}$$

$$\nabla(\rho f.\,ui.\,\varepsilon) = \nabla(\rho f.\,Di, e.\,\nabla xi) + (1-\varepsilon)\rho Mi \sum_{j} Vij\ rj + Si \tag{3}$$

The CFD model also needed to apply additional equations to calculate some of the parameters found in Eqs. (1 to 3), as explained in the next section. based on the Ergun equation (Eq. (4)) was found to be:

$$\beta = \frac{150\mu f(1-\varepsilon)\text{^}2}{\varepsilon\text{^}3dp\text{^}2} + \frac{1.75(1-\varepsilon)\rho f}{\varepsilon\text{^}3dp}|u| \tag{4}$$

is the permeation the flux of the permeation (Ji) of the component i, can calculate by

$$Ji = Pei * (Pi, retentate - Pi, permeate) \tag{5}$$

Where $Pei* = \frac{Pei}{\delta}$ is i-species permeate

Use the Arrhenius equation to calculate Pei

$$Pei = Po, i \exp\left(-\frac{Ea, i}{RT}\right) \tag{6}$$

The recovery of flare gas is shown in Figure 2 below for the "catalytic membrane reactor". In this study, the membrane reactor model is solved under the straightforward conditions of negligible axial diffusion, steady-state conditions, negligible radial convective mass transfer, and substantial heat conduction of the membrane material [19].

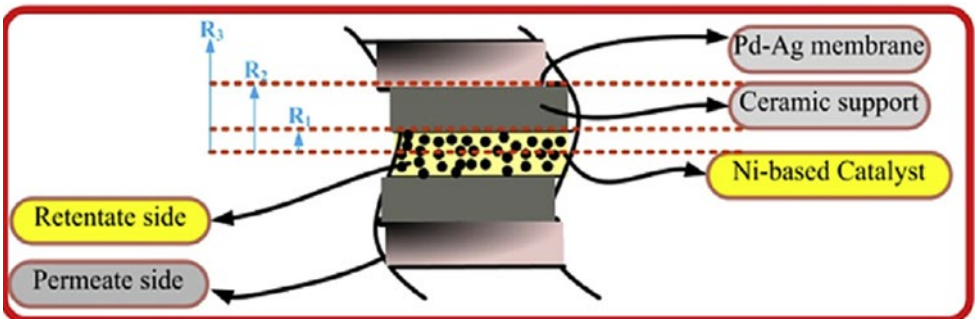

Fig.2 CMR for gas flare recovery [19].

The implicit finite element method is used to solve the model equations numerically, and the governing equations have been introduced to the MATLAB programming for the purpose of model development.

The Tube Side the Governing Equations

In order to account for the mass transfer convective in the axial and radial direction, chemical reactions, diffusion direction, and the mass balance for each component in (tube side: 0 to R_1) is given:

$$\frac{\partial(u_z^t)}{\partial z} = \varepsilon^t \frac{1}{r}\frac{\delta}{\delta r}\left(r D_{e,i}^t \frac{\partial C_i^t}{\partial r}\right) + P_{cat.}^t(1-\varepsilon^t) \times \sum_{j=1}^{N_R} \gamma_{ij\,rj} \tag{7}$$

The equation of overall heat transfer

$$\rho_G^t \, cp \, u_z^t \frac{\partial T^t}{\partial z} = \frac{1}{r}\frac{\partial}{\partial r}\left(\lambda_{ef}^t r \frac{\partial T^t}{\partial r}\right) P_{cat.}^t(1-\varepsilon^t) \times \sum_{j=1}^{N_R} r_{j\,(-\Delta H_j)} \tag{8}$$

The flux of H_2 permeation flux through the membrane

$$J_{H_2} = \frac{P_{eo}.\exp\left(-\frac{E_a}{RT}\right)\left[\sqrt{P_{H_2}^c} - \sqrt{P_{H_2}^s}\right]}{\delta} \tag{9}$$

The Shell Side the Governing Equations

$$\frac{\partial(u_z^s C_z^s)}{\partial z} = 0 \tag{10}$$

$$\frac{\partial u_z^s}{\partial z} = \frac{2R_2 RT_O}{P_O(R_3^2 - R_2^2)} \frac{Q_O}{\delta}\left[\sqrt{P^c}H_2 - \sqrt{P^s H_2}\right] \tag{11}$$

Bian, Z., et al;[20], utilized simulations of the enclosed equations mentioned in table 4 and their solution using the COMSOL software to explore the behavior of a catalytic membrane reactor for the dry reforming of methane.

Table 4 Equations of Two-dimensional CFD model [20].

Permeate side	Retentate side
Continuity equation	
$\nabla(\rho v^{\rightarrow}) = 0$	$\boldsymbol{\nabla(\varepsilon\rho v) = 0}$
$\rho = \frac{P}{RT\sum_i \frac{w_i}{M_i}}$	$\boldsymbol{\rho = \frac{P}{RT\sum_i \frac{W_i}{M_i}}}$
Momentum equation	
$\rho v^{\rightarrow}.\nabla v^{\rightarrow} = -\nabla[P + \mu(\nabla v^{\rightarrow} + \left(\nabla v^{\rightarrow}\right)^T - \frac{2\mu}{3}(\nabla v^{\rightarrow})\right]$	$\boldsymbol{v^{\rightarrow} = -\frac{K}{\mu}\nabla P}$
Mass equation	
$\nabla.j_i^{\rightarrow} + \rho(v^{\rightarrow}.\nabla)w_i = 0$	$\boldsymbol{\nabla.j_i^{\rightarrow} + \rho(v^{\rightarrow}.\nabla)w_i = R_i}$
$j_i^{\rightarrow} = -\rho w_i \sum_j D_{ij}[\nabla x_i + (x_j - w_j)\frac{\nabla P}{P}]$	$\boldsymbol{j_i^{\rightarrow} = -\rho w_i \sum_j D_{ijeff}[\nabla x_i + (x_j - w_j)\frac{\nabla P}{P}]}$
$x_i = \frac{w_k}{M_k}.(\sum_i \frac{w_k}{M_k})^{-1}$	$\boldsymbol{x_i = \frac{w_k}{M_k}.(\sum_i \frac{w_k}{M_k})^{-1}}$

The primary goal of this paper is to review theoretical research on methods of producing hydrogen using membrane reactor modeling and simulation. This review will focus on the best membrane to use depending on the amount of hydrogen permeability, which is influenced by a number of different factors, including temperature, pressure, catalyst type, feed rate, sweep gas flow rate, feed purity, and reactor type depending on how the catalyst is arranged in the membrane.

Grace, J., et al;[21], used SMR equilibrium modeling with oxygen and hydrogen withdrawals. Water is a necessary reactant in this process because it is a byproduct of the oxidation reactions needed to create autothermal conditions. The operation at lower temperatures, lower H2O/CH4 and greater pressures are made possible by the permeable membranes and O2 to steam methane reforming reactors.

Iulianelli, A., et al;[22], produced greater methane and hydrogen yield conversion than traditional FBR rates under the same conditions when simulating steam methane reforming in a dense Pd-Ag MR packed with a nickel-based catalyst at low pressure (1.0-3.0 bar) and temperatures ranging from 400 to 500 °C. 70% of pure hydrogen may be produced in the packed bed membrane reactor without the addition of CO or CO2 using sweep gas on the permeate side.

Coronel, L., et al;[23], investigates this FBCMR using numerical simulations and a 2-dimensional model with mass, momentum, and energy balances. The fixed bed is believed to be formed using Ru/SiO2 catalyst particles that are specifically made for steam reformation at low H2O/C and temperature ratios. A composite Pd membrane was proposed for H2 permeation. After the model was verified by experimental data, a comparison of a straightforward 1-dimentional model to a more intricate 2-dimentional model was made to determine how well it represented the membrane reactor. The effectiveness of a simplified 1-dinentional model to simulate the membrane reactor was assessed and discussed in contrast. Pressure, inlet temperature, steam excess, space velocity, and the rate of sweep gas in the permeate are the primary operational parameters.

Chein, R., et al;[24], Utilizing a 3-dimensional mathematical model, a water gas shift reaction in MR was employed to mimic the synthesis of H2 from coal-derived syngas. The working temperature at the gasifier exit is 900 °C, which is the typical syngas temperature. The productivity of the reactor was investigated in relation to the (H2O/C) ratio, reactant residence time, reactant composition, sweep gas flow rate, and membrane permeance. H2 recovery and CO conversion were utilized to evaluate the reactor's performance. Increases in the H2O/C ratio, membrane permeance, and sweep gas flow rate were noted. Limiting values for H2 recovery and CO conversion were found when these parameters were raised further, which improved the reactor's performance. Additionally, the mathematical results demonstrated that the reactor's efficiency decreased as the CO_2 content climbed.

Chompupun, K., et al; [25], used a 3-dimensional model for the catalytic membrane reactor in the COMSOL Multiphysics program that takes into account energy, momentum, and the effects of multicomponent diffusion. We examine the best geometrical arrangement for the suggested design. There are ideas offered for the reactor's design. It has been proven that the surface area-to-reactor volume ratio of the design with the best membrane, 255 m2/m3, is correlated with a Peclet number-Damkohler product that is near to 1.

Lee, B., et al;[26], utilized a CFD model for the dry reforming of methane (CO2 reforming) in conventional packed bed reactors (PBR) and membrane reactors (MR), with the heating tube serving as both types of reactors' main heat source. An unusual packed bed reactor and a membrane reactor have both been explored to see how reactor geometry affects temperature and profiles of hydrogen and methane concentrations. The membrane centre distances in an MR were 0.028 m, 0.03 m, 0.033 m, 0.035 m, 0.038 m, 0.04 m, 0.042 m, 0.044 m, and 0.045 m from the reactor centre. Using COMSOL Multiphysics modelling.

Cifuentes, A., et al;[27], used a 3-dimensional CFD non-isothermal model with mass transfer constraints.Under different pressure feed load and temperature circumstances, it was projected that reverse water-gas shift, methanation, and steam methan reforming would occur. The model evaluated and simulated the catalytic membrane reactor under various operating conditions. $PdZn/ZnAl_2O_4/Al_2O_3$ catalyst pellets are packed during the steam reforming of methanol with a steam to carbon ratio of 1 (S/C = 1).

Table 5 Summarized of Membrane Reactor Modeling and Simulation Studies.

No.	Reactor - type	Condition	Feed	Catalyst	Production Method	Softewaer	Configuration	Ref.
1	MR (Pd-Ag)	T=513k, P=10bar, Isothermal	methanol	Ni/Al_2O_3	Steam Reforming	COMSOL multiphy-sics	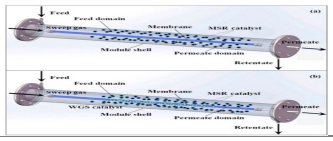	[18]
2	FBMR (Pd)	T=580C, P=2.9MPa Isothermal,	Methane	Ni/Al_2O_3	Steam Reforming	RAND algorithm	-	[21]
3	CMR (dense Pd–Ag)	T=400 and 500 °C, P=(1.0–3.0 bar), Isothermal	Methane	Ni/Al_2O_3	Steam Reforming	fourth-order Rungee Kutta method	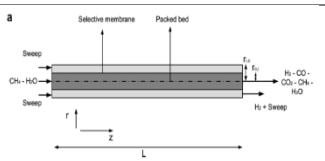	[22]
4	Tubular MR (dense Pd–Ag)	T=823 K, P=101, 325 Pa, Isothermal	Methane	Rh/La_2O_3, $Rh/La_2O_3 – SiO_2$	Dry Reforming	MathCad ™ Profes-sional software	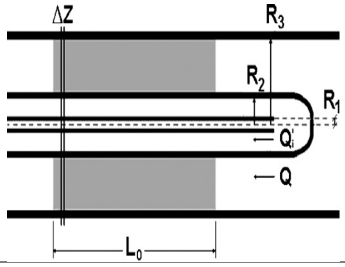	[23]
4	MR (Pd)	T=900C, P= 1.013×10^5Pa, Isothermal	Methane	Ni/Al_2O_3	Steam Reforming	COMSOL multi-physics	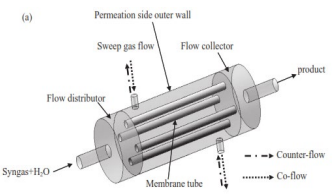	[24]

5	CMR (Pd)	T= 723–823K., Isothermal	Methane	Ni/Al_2O_3	Steam Reforming	COMSOL multiphy-sics	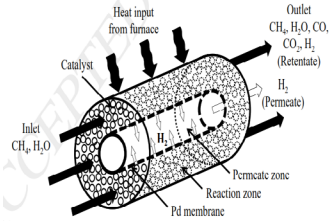	[25]
6	MR(Pd)	T=923 K,Non-isothermal	Methane	Rh/Al_2O_3	CO_2 Reforming	COMSOL multiphy-sics	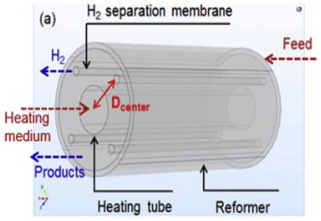	[26]
7	CMR dense Pd–Ag	Isothermal	Methanol	$PdZn/ZnAl_2O_4/Al_2O_3$	Steam Reforming	COMSOL multiphy-sics	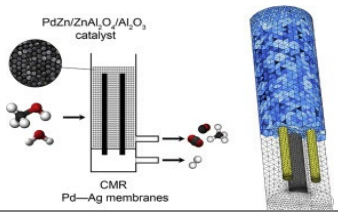	[27]
8	Tubular MR dense Pd–Ag	T=673 K,P=1 atm, Isothermal	Methane	$Pt(0.6)/La_2O_3$ (27) SiO_2	Steam Reforming	COMSOL multiphy-sics	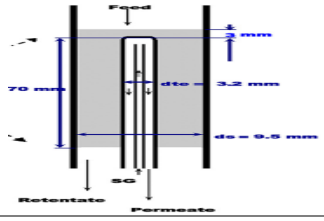	[28]
9	MR(Pd)	T=673–863K, P=101KP, Non-isothermal	Methane	Ni/Al_2O_3	Steam Reforming	ANSYS FLUENT	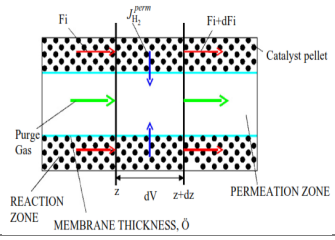	[29]
10	PBMR Porous Vycor Glass	T=550 K,P=1.013×10^{5}PaNon-isothermal,	Cyclohexane.	Pt/Al_2O_3	Dehydroge-nation	ANSYS FLUENT	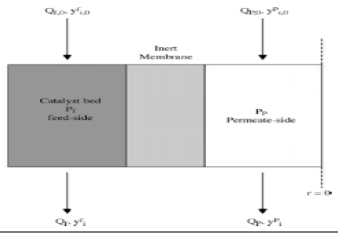	[30]
11	TCMRPd-Ag	T=503K, P=1.013×10^{5}Pa, Isothermal	Cyclohexane	Ni/Al_2O_3	Dehydrogena-tion	ANSYS FLUENT	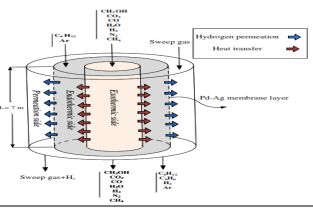	[31]

12	BMR, Pd	T=823K, P=4to10bar, Isothermal	methane	Ni/Mg2Al 4 O	Steam Reforming	ANSYS FLUENT	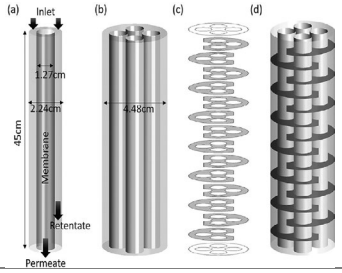	[32]
13	MR(Pd)	Isothermal	methane	Ni-based catalyst	Steam Reforming	ANSYS FLUENT	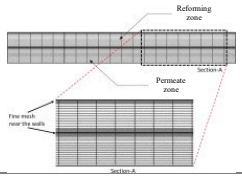	[33]
14	MR Pd-Ru	T=673-1273 K, P=200Kpa, Isothermal	methane	Ni/Al2O3	Steam Reforming	ANSYS FLUENT	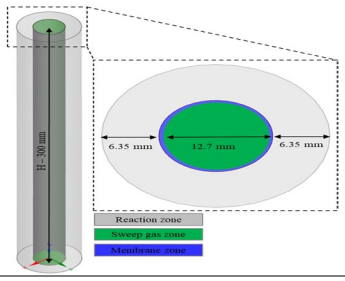	[34]
15	SEMR (Pd)	T=500K, Poutlet= 0.3Mpa, Isothermal	methane	Ni/Al2O3	Steam Reforming	ANSYS FLUENT	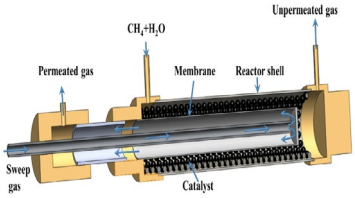	[35]
16	CMR Pd-Ru	T=853K, Poutlet=0.8-3.5Mpa, Isothermal	methane	Ni/Al2O3	Steam Reforming	ANSYS FLUENT	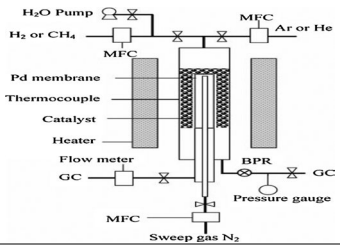	[36]
17	TCMR (Pd)	T=400-900K, Poutlet= 0.8-3.5Mpa, Isothermal	methane	Ni/MgO–Al2O3	Steam Reforming	ANSYS FLUENT	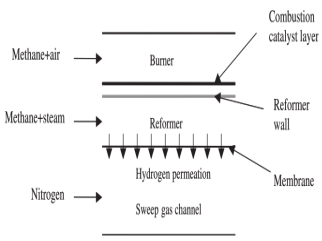	[37]
18	FBMR (Pd)	T=350-500 C, P= 1.013× 10^5Pa, Isothermal	Methane	Ru/SiO_2	Steam Reforming	COMSOL multiphy-sics	-	[7, 38]

19	Tubular MR (Pd-Au)	T=500C, P=5bar, Isothermal	Ethanol	Pt/Ni-CeO_2	Steam Reforming	COMSOL multiphy-sics	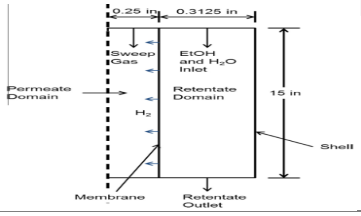	[39]
20	Multi-tubular MR(Pd)	T=400C, P=25 bar, Isothermal	Methane	Ni/Al_2O_3	Steam Reforming	ASPEN Plus	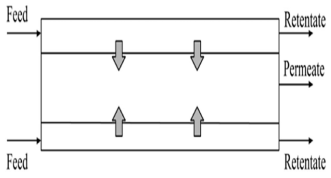	[40]
21	CMR	T=543.15 K,P= 1.013 bar	Methylcycloh exane	Ni/Al_2O_3	Dehydroge-nation	COMSOL multip-hysics	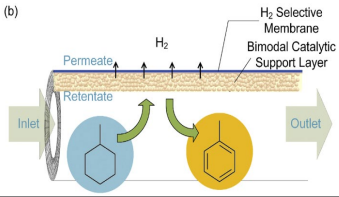	[41]
22	FBMR(Pd)	T=923 K, P= 1.013 bar, Isothermal	Methane	Ni/Al_2O_3	Steam Reforming	fourth-order Rungee Kutta method	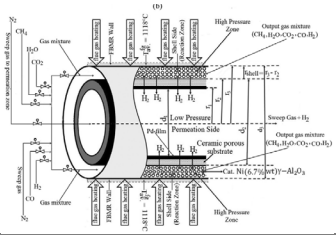	[42]
23	PBMR (Pd-Ag)	T=473 K Non-isothermal,	Methanol	Ni/Al_2O_3	Steam Reforming	ANSYS FLUENT	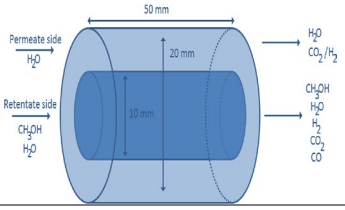	[43]
24	MR Ceramic	T=773 K, P= 2.53×10^5 Pa, Isothermal	methane	Ni/Al_2O_3	Steam Reforming	ANSYS FLUENT	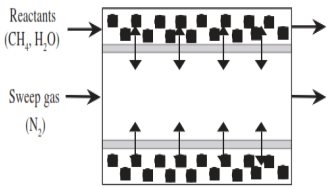	[44]
25	CMR (Pd)	T=450–700°C0, P=1325 Pa, Non-isothermal	methane	Ni/Al2O3	Dry Reforming	ANSYS FLUENT	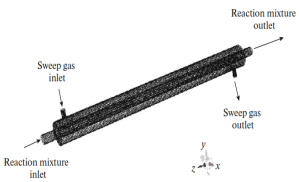	[45]
26	MR(Pd)	T= 673-773 K, P=1325 Pa, Non-isothermal	glycerol	Ni/Al2O3	Steam Reforming	MATLAB software	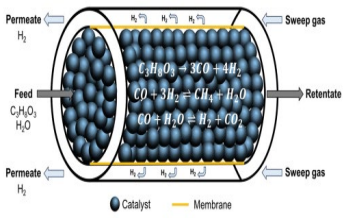	[46]

27	MR(Pd)	T= 350–500°C, P= 0.1 MPa Isothermal,	Ethanol	Ni/Al2O3	Steam Reforming	COMSOL multiphy-sics	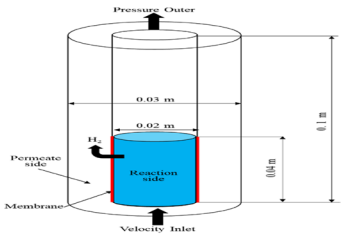	[47]
28	MR(Pd)	Isothermal	Methane	Ni/Al2O3	Steam Refor-ming	COMSOL multiphy-sics	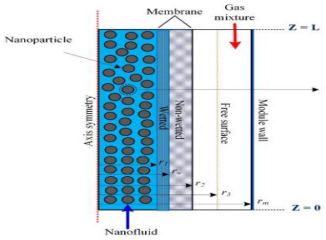	[48]
29	MR(Pd)	T=525 C Isothermal,	Methane	$(Pt_{(3)}Ni_{(10)}/CeO2)$	Steam Reforming	COMSOL multiphy-sics	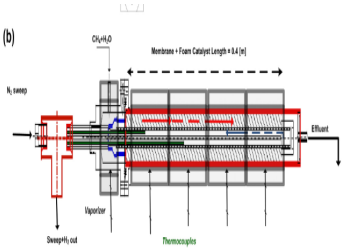	[49]

Summary

The evaluation of the aforementioned study led us to the following conclusions:

1. Traditional catalytic reactors cannot produce H_2 as efficiently as catalytic membrane reactors (CMR) can (TCR).
2. The steam reforming process (SR) is a further method for producing H_2 that uses sweep gas to obtain H_2 from the permit side and natural gas as the feed to the reactor.
3. The best membrane material with a high rate of H_2 permeability across the membrane is a palladium-based alloy; silica is often employed as a backup option to palladium metal.
4. Simulated the experimental data using the COMSOL software, MATLAB, and Finite Element Method in order to compare the modeling and simulation findings with the actual results and to investigate the mass, momentum, and energy aspects of the process.

Nomenclature

ρ_f	density fluid kg/m^3.
ε	void fraction of the catalytic bed.
Si	sink/source that indicating the flux of permeation of the i component through the membrane.
B	the coefficient of friction.
Xi	fraction of mass component i.
r	Radial coordinate, m.
Di,e,Mi	the coefficient of diffusion and molar weight of the i-component, respectively.
rj	Rate of reaction j, mol/kgcat.s.
δ	Membrane thickness, m.
Pei	Permeability coefficient, mol /s.cm. atm$^{0.5}$.
Pe0,i	constant coefficient.
Ea,i	Apparent activation energy for membrane, J / mol.
R	Universal gas constant, kPa. m^3/mol.K.
T	Temperature, K.

A	Cross-sectional area of reactor m^2.
$v^{\wedge}\rightarrow$	vector of velocity of gas mixture.
ΔH_i	Heat of adsorption for surface species i or heat of reaction for formation of surface species i, kJ /mol.
u	Gas velocity, m/s.
P	Total pressure, bar.
M_i	Molecular weight of ith compound, g/ mole.
C_i	Concentration of i species, kmol / m^3.
μ	Gas viscosity, kg /m.s .
ρ_g	Density of gas, kg / m^3.
ρ_{cat}	Density of the catalyst bed, kg/ m^3.
R_1	Tube radius, m.
R_2	Shell radius, m.
r_{cat}	Catalyst size, mm
D_e	Effective coefficient of radial diffusion of component I m^2/s.
κ	Packed bed permeability, m^2.
D_{ij}	Binary gas diffusivity, m^2/s.
λ_{ij}	Stoichiometric coefficient.

Subscripts

CMR	Catalytic Membrane Reactor.
MSR	Methane Steam reforming.
S	Shell side.
T	Tube side.
f	Fluid.
CFD	Computational fluid dynamics
Pd	palladium
MR	Membrane reactor
SCR	Steam to carbon ratio

References

[1] S. P. Katikaneni et al., "Catalytic Membrane Reactor for Hydrogen Production from Liquid Petroleum Fuels: Bench Scale Studies," Saudi Aramco Journal of Technology, p. 35, 2008.

[2] M. Martino, C. Ruocco, E. Meloni, P. Pullumbi, and V. Palma, "Main hydrogen production processes: An overview," Catalysts, vol. 11, no. 5, p. 547, 2021.

[3] S. Z. Baykara, "Hydrogen: A brief overview on its sources, production and environmental impact," International Journal of Hydrogen Energy, vol. 43, no. 23, pp. 10605-10614, 2018.

[4] G. Cipriani et al., "Perspective on hydrogen energy carrier and its automotive applications," International Journal of Hydrogen Energy, vol. 39, no. 16, pp. 8482-8494, 2014.

[5] S. S. Kumar and V. Himabindu, "Hydrogen production by PEM water electrolysis–A review," Materials Science for Energy Technologies, vol. 2, no. 3, pp. 442-454, 2019.

[6] T. Yusaf et al., "Sustainable Aviation—Hydrogen Is the Future. Sustainability 2022, 14, 548," ed: s Note: MDPI stays neutral with regard to jurisdictional claims in published …, 2022.

[7] V. Spallina et al., "Direct route from ethanol to pure hydrogen through autothermal reforming in a membrane reactor: Experimental demonstration, reactor modelling and design," Energy, vol. 143, pp. 666-681, 2018.

[8] N. Pal, M. Agarwal, K. Maheshwari, and Y. S. Solanki, "A review on types, fabrication and support material of hydrogen separation membrane," Materials Today: Proceedings, vol. 28, pp. 1386-1391, 2020.

[9] C. Z. Liang, T.-S. Chung, and J.-Y. Lai, "A review of polymeric composite membranes for gas separation and energy production," Progress in Polymer Science, vol. 97, p. 101141, 2019.

[10] Y. Vijay, S. Wate, N. Acharya, and J. Garg, "The titanium-coated polymeric membranes for hydrogen recovery," International journal of hydrogen energy, vol. 27, no. 9, pp. 905-908, 2002.

[11] S. K. Gade, P. M. Thoen, and J. D. Way, "Unsupported palladium alloy foil membranes fabricated by electroless plating," Journal of Membrane Science, vol. 316, no. 1-2, pp. 112-118, 2008.

[12] M. Weber et al., "Hydrogen selective palladium-alumina composite membranes prepared by Atomic Layer Deposition," Journal of membrane Science, vol. 596, p. 117701, 2020.

[13] D. P. Tanaka, J. Medrano, J. V. Sole, and F. Gallucci, "Metallic membranes for hydrogen separation," in Current trends and future developments on (bio-) membranes: Elsevier, 2020, pp. 1-29.

[14] L. Roses, G. Manzolini, S. Campanari, E. De Wit, and M. Walter, "Techno-economic assessment of membrane reactor technologies for pure hydrogen production for fuel cell vehicle fleets," Energy & fuels, vol. 27, no. 8, pp. 4423-4431, 2013.

[15] S. Paglieri and J. Way, "Innovations in palladium membrane research," Separation and Purification Methods, vol. 31, no. 1, pp. 1-169, 2002.

[16] J. Sanchez and T. T. Tsotsis, "Current developments and future research in catalytic membrane reactors," in Membrane Science and Technology, vol. 4: Elsevier, 1996, pp. 529-568.

[17] F. Gallucci, L. Paturzo, and A. Basile, "A simulation study of the steam reforming of methane in a dense tubular membrane reactor," International Journal of Hydrogen Energy, vol. 29, no. 6, pp. 611-617, 2004.

[18] K. Ghasemzadeh, J. Harasi, T. Amiri, A. Basile, and A. Iulianelli, "Methanol steam reforming for hydrogen generation: A comparative modeling study between silica and Pd-based membrane reactors by CFD method," Fuel Processing Technology, vol. 199, p. 106273, 2020.

[19] M. Saidi, "Application of catalytic membrane reactor for pure hydrogen production by flare gas recovery as a novel approach," International Journal of Hydrogen Energy, vol. 43, no. 31, pp. 14834-14847, 2018.

[20] Z. Bian et al., "CFD simulation of a hydrogen-permeable membrane reactor for CO2 reforming of CH4: the interplay of the reaction and hydrogen permeation," Energy & Fuels, vol. 34, no. 10, pp. 12366-12378, 2020.

[21] J. R. Grace, X. Li, and C. J. Lim, "Equilibrium modelling of catalytic steam reforming of methane in membrane reactors with oxygen addition," Catalysis today, vol. 64, no. 3-4, pp. 141-149, 2001.

[22] A. Iulianelli et al., "H2 production by low pressure methane steam reforming in a Pd–Ag membrane reactor over a Ni-based catalyst: experimental and modeling," International journal of hydrogen energy, vol. 35, no. 20, pp. 11514-11524, 2010.

[23] L. Coronel, J. Múnera, E. A. Lombardo, and L. M. Cornaglia, "Pd based membrane reactor for ultra pure hydrogen production through the dry reforming of methane. Experimental and modeling studies," Applied Catalysis A: General, vol. 400, no. 1-2, pp. 185-194, 2011.

[24] R. Chein, Y. Chen, Y. Chyou, and J. Chung, "Three-dimensional numerical modeling on high pressure membrane reactors for high temperature water-gas shift reaction," International journal of hydrogen energy, vol. 39, no. 28, pp. 15517-15529, 2014.

[25] T. Chompupun, S. Limtrakul, T. Vatanatham, C. Kanhari, and P. A. Ramachandran, "Experiments, modeling and scaling-up of membrane reactors for hydrogen production via steam methane reforming," Chemical Engineering and Processing-Process Intensification, vol. 134, pp. 124-140, 2018.

[26] B. Lee et al., "CO2 reforming of methane for H2 production in a membrane reactor as CO2 utilization: computational fluid dynamics studies with a reactor geometry," International Journal of Hydrogen Energy, vol. 44, no. 4, pp. 2298-2311, 2019.

[27] A. Cifuentes, L. Soler, R. Torres, and J. Llorca, "Methanol steam reforming over PdZn/ZnAl2O4/Al2O3 in a catalytic membrane reactor: An experimental and modelling study," International Journal of Hydrogen Energy, vol. 47, no. 22, pp. 11574-11588, 2022.

[28] C. A. Cornaglia, M. E. Adrover, J. F. Múnera, M. N. Pedernera, D. O. Borio, and E. A. Lombardo, "Production of ultrapure hydrogen in a Pd–Ag membrane reactor using noble metals supported on La–Si oxides. Heterogeneous modeling for the water gas shift reaction," International journal of hydrogen energy, vol. 38, no. 25, pp. 10485-10493, 2013.

[29] M. De Falco, L. Di Paola, and L. Marrelli, "Heat transfer and hydrogen permeability in modelling industrial membrane reactors for methane steam reforming," International Journal of Hydrogen Energy, vol. 32, no. 14, pp. 2902-2913, 2007.

[30] H.-S. Yang and C.-T. Chou, "Non-isothermal simulation of cyclohexane dehydrogenation in an inert membrane reactor with catalytic pellets in the feed-side chamber," Journal of the Chinese Institute of Chemical Engineers, vol. 39, no. 3, pp. 227-235, 2008.

[31] M. Rahimpour and M. Bayat, "Production of ultrapure hydrogen via utilizing fluidization concept from coupling of methanol and benzene synthesis in a hydrogen-permselective membrane reactor," International journal of hydrogen energy, vol. 36, no. 11, pp. 6616-6627, 2011.

[32] H. Choi et al., "CFD analysis and scale up of a baffled membrane reactor for hydrogen production by steam methane reforming," Computers & Chemical Engineering, vol. 165, p. 107912, 2022.

[33] R. Ben-Mansour et al., "Comprehensive parametric investigation of methane reforming and hydrogen separation using a CFD model," Energy Conversion and Management, vol. 249, p. 114838, 2021.

[34] M. Upadhyay, H. Lee, A. Kim, S.-h. Lee, and H. Lim, "CFD simulation of methane steam reforming in a membrane reactor: Performance characteristics over range of operating window," International Journal of Hydrogen Energy, vol. 46, no. 59, pp. 30402-30411, 2021.

[35] G. Ji, M. Zhao, and G. Wang, "Computational fluid dynamic simulation of a sorption-enhanced palladium membrane reactor for enhancing hydrogen production from methane steam reforming," Energy, vol. 147, pp. 884-895, 2018.

[36] H. W. A. El Hawa, S. N. Paglieri, C. C. Morris, A. Harale, and J. D. Way, "Application of a Pd–Ru composite membrane to hydrogen production in a high temperature membrane reactor," Separation and Purification Technology, vol. 147, pp. 388-397, 2015.

[37] K. S. Patel and A. K. Sunol, "Modeling and simulation of methane steam reforming in a thermally coupled membrane reactor," International Journal of Hydrogen Energy, vol. 32, no. 13, pp. 2344-2358, 2007.

[38] P. Marín, Y. Patiño, F. V. Díez, and S. Ordóñez, "Modelling of hydrogen perm-selective membrane reactors for catalytic methane steam reforming," International journal of hydrogen energy, vol. 37, no. 23, pp. 18433-18445, 2012.

[39] R. Ma, B. Castro-Dominguez, I. P. Mardilovich, A. G. Dixon, and Y. H. Ma, "Experimental and simulation studies of the production of renewable hydrogen through ethanol steam reforming in a large-scale catalytic membrane reactor," Chemical engineering journal, vol. 303, pp. 302-313, 2016.

[40] A. Shafiee, M. Arab, Z. Lai, Z. Liu, and A. Abbas, "Modelling and sequential simulation of multi-tubular metallic membrane and techno-economics of a hydrogen production process employing thin-layer membrane reactor," international journal of hydrogen energy, vol. 41, no. 42, pp. 19081-19097, 2016.

[41] Y.-R. Chen, T. Tsuru, and D.-Y. Kang, "Simulation and design of catalytic membrane reactor for hydrogen production via methylcyclohexane dehydrogenation," International Journal of Hydrogen Energy, vol. 42, no. 42, pp. 26296-26307, 2017.

[42] B. M. Cruz and J. D. da Silva, "A two-dimensional mathematical model for the catalytic steam reforming of methane in both conventional fixed-bed and fixed-bed membrane reactors for the Production of hydrogen," International Journal of Hydrogen Energy, vol. 42, no. 37, pp. 23670-23690, 2017.

[43] P. Ribeirinha, M. Abdollahzadeh, M. Boaventura, and A. Mendes, "H2 production with low carbon content via MSR in packed bed membrane reactors for high-temperature polymeric electrolyte membrane fuel cell," Applied Energy, vol. 188, pp. 409-419, 2017.

[44] W. Yu et al., "Simulation of a porous ceramic membrane reactor for hydrogen production," International journal of hydrogen energy, vol. 30, no. 10, pp. 1071-1079, 2005.

[45] Y. Benguerba, M. Virginie, C. Dumas, and B. Ernst, "Computational fluid dynamics study of the dry reforming of methane over Ni/Al 2 O 3 catalyst in a membrane reactor. Coke deposition," Kinetics and Catalysis, vol. 58, pp. 328-338, 2017.

[46] M. S. Macedo, M. Soria, and L. M. Madeira, "Glycerol steam reforming for hydrogen production: Traditional versus membrane reactor," International Journal of Hydrogen Energy, vol. 44, no. 45, pp. 24719-24732, 2019.

[47] X. Yang, S. Wang, B. Li, Y. He, and H. Liu, "Performance of ethanol steam reforming in a membrane-assisted packed bed reactor using multiscale modelling," Fuel, vol. 274, p. 117829, 2020.

[48] N. Ghasem, "Modeling and simulation of CO2 absorption enhancement in hollow-fiber membrane contactors using CNT–water-based nanofluids," Journal of Membrane Science and Research, vol. 5, no. 4, pp. 295-302, 2019.

[49] M. Patrascu and M. Sheintuch, "On-site pure hydrogen production by methane steam reforming in high flux membrane reactor: Experimental validation, model predictions and membrane inhibition," Chemical Engineering Journal, vol. 262, pp. 862-874, 2015.